Substate Populations and Nuclear Polarization Produced by Inelastic Alpha-Particle Scattering on Carbon-12*†‡

T. D. HAYWARD§ AND F. H. SCHMIDT
Department of Physics, University of Washington, Seattle, Washington 98105
(Received 23 September 1969)

We have measured the normalized α-γ angular correlation in the reaction plane for excitation of the 4.44-MeV, 2^+ state of ^{12}C at 22.750 MeV. These data yield the relative populations $(a_m)^2$ of the three magnetic substates referred to the normal to the reaction plane. The ambiguity between $(a_{+2})^2$ and $(a_{-2})^2$ was resolved by coincidence measurements of the circular polarization of deexcitation γ rays emitted near the normal to the reaction plane. The inelastic scattering process can then be dissected into partial differential cross sections σ_m to the substates. The results show that each σ_m has a different angular dependence. σ_0 has the most regular and pronounced diffractionlike structure, σ_{-2} dominates out to 75°, and σ_{+2} dominates thereafter. Thus, the excited nuclei spin in the sense of classical hard-sphere scattering with friction out to $\approx$75°, and in the reverse sense from $\approx$75° to $\approx$170°. The nuclear polarization exhibits an oscillatory character as a function of angle. Comparison of the results with diffraction-model calculations, and with distorted-wave Born-approximation calculations, is poor. In principle, the experimental method, though difficult, could be applied to nuclei which are more accurately described by nuclear models than is ^{12}C.

I. INTRODUCTION

THE scattering of α particles has long been a useful technique for the study of nuclear properties. Although deviations from Rutherford scattering had been observed much earlier, these became very pronounced[1] at energies available from particle accelerators. Blair[2] and others interpreted the results in terms of a strong absorption model.

The familiar diffractionlike angular distributions, first observed for elastic scattering, were reported for inelastic scattering by Gugelot and Rickey[3]; since then numerous other groups have made similar studies in ever greater detail. The strong absorption model was highly successful in explaining the chief features of elastic scattering; extensions of the model to collective excitations in inelastic scattering predicted the so-called Blair phase rule.[4] The recent experiments by Hendrie *et al.*,[5] and by Fernandez and Blair,[6] have carried the technique of differential cross-section measurements to a high degree of sophistication.

The earliest work on the angular correlation between inelastically scattered α particles and deexcitation γ rays was done by Shook.[7] More extensive experiments have been reported by Hendrie *et al.*,[8] McDaniels *et al.*,[9] Eidson *et al.*,[10] and by others.[11] The angular correlation method yielded additional details of the inelastic scattering process and generated various new theoretical treatments.[12]

The purpose of the present paper is to report the successful application of extensions of the angular correlation technique, which lead to further detailed dissections of the inelastic scattering process into its component parts. The extensions consist of absolute, rather than relative, measurements of the angular correlation functions, and determinations of the sign, or sense, of circularly polarized deexcitation γ rays emitted in directions near the normal to the plane of the particle reaction.

Efforts to detect the circular polarization of γ rays following inelastic α-particle scattering were begun in 1959, and abandoned[13] when it was shown that, with the 42-MeV α beam from the University of Washington 60-in. cyclotron, the length of time required to obtain meaningful results would be excessive.

Interest in the experiment was rekindled by the angular correlation studies of Eidson *et al.*,[10] who used the 22.5-MeV beam of the Indiana cyclotron, the results of which showed that the residual $^{12}C^*(4.44)$

* Work supported in part by U.S. Atomic Energy Commission.
† This work was submitted by one of us (T.D.H.) in partial fulfillment of the requirements for the Ph.D. degree at the University of Washington.
‡ Preliminary results have been presented in abstract form: T. D. Hayward, D. M. Patterson, F. H. Schmidt, and J. R. Tesmer, Bull. Am. Phys. Soc. **13,** 1448 (1968); F. H. Schmidt, T. D. Hayward, D. M. Patterson, and J. R. Tesmer, *ibid.* **13,** 1448 (1968).
§ Present address: Duke University, Durham, N.C.
[1] G. W. Farwell and H. E. Wegner, Phys. Rev. **93,** 356 (1954); **95,** 664 (1954); **95,** 1212 (1954); R. M. Eisberg and C. E. Porter, Rev. Mod. Phys. **33,** 190 (1961).
[2] J. S. Blair, Phys. Rev. **95,** 604 (1954); **95,** 1218 (1954).
[3] P. C. Gugelot and M. Rickey, Phys. Rev. **101,** 1613 (1956).
[4] J. S. Blair, Phys. Rev. **115,** 928 (1959).
[5] D. L. Hendrie, N. K. Glendenning, B. G. Harvey, O. N. Jarvis, H. H. Duhm, J. Mahoney, and J. Saudinos, in Proceedings of the International Conference on Nuclear Structure, Tokyo, 1967 (unpublished), p. 306.
[6] B. Fernadez and J. S. Blair, Phys. Rev. C **1,** 523 (1970).
[7] G. B. Shook, Phys. Rev. **114,** 310 (1959).
[8] D. L. Hendrie and D. K. McDaniels, Bull. Am. Phys. Soc. **7,** 270 (1962).
[9] D. K. McDaniels, D. L. Hendrie, R. H. Bassel, and G. R Satchler, Phys. Letters **1,** 295 (1962).
[10] W. Eidson, J. G. Cramer, Jr., D. E. Blatchley, and R. D. Bent, Nucl. Phys. **55,** 613 (1964).
[11] D. E. Blatchley and R. D. Bent, Nucl. Phys. **61,** 641 (1965); W. W. Eidson, J. G. Cramer, Jr., and G. P. Eckley, Phys. Letters **18,** 34 (1965); S. S. Klein, A. Meiser, and O. J. Poppema, Nucl. Phys. **A121,** 422 (1968).
[12] D. R. Inglis, Phys. Letters **10,** 336 (1964); Phys. Rev. **142,** B591 (1966); B. J. Verhaar and L. D. Tolsma, Phys. Letters **17,** 928 (1965); Nucl. Phys. **A90,** 612 (1967).
[13] Annual Progress Report, Cyclotron Research, University of Washington, 1959, 1960, and 1961 (unpublished).

nuclei were indeed polarized. The sign of the polarization was not determined. Acquisition of a Tandem Van de Graaff accelerator[14] by the University of Washington reopened the possibility of conducting the experiments. These two considerations were sufficient to give us courage to proceed.

The theory of the method is outlined in Sec. II. Since some of our experimental methods and data analysis are relatively new, we report these in detail in Secs. III and V. We have successfully applied these techniques to the $^{12}C(\alpha, \alpha'\gamma)^{12}C^*$ (4.44) reaction at 22.750-MeV bombarding energy. Although ^{12}C is well-known for its recalcitrant ability to defy theoretical interpretation,[15] we chose it nevertheless for its pleasant experimental aspects—a large inelastic cross section to the first excited state, and low background radiation. Our results, described in Sec. VI, show that the three partial cross sections to the substates $m=0, \pm 2$ exhibit different diffractionlike angular distributions. The $m=0$ cross section is the most regular. The difference between the $m=+2$ and -2 gives rise to nuclear polarization, which itself shows an oscillatory variation with scattering angle. The sense of the polarization is that to be expected for classical hard-sphere scattering with contact friction for angles from $\approx 20°$ to $\approx 75°$, but the reverse is true from $\approx 75°$ to $\approx 170°$. In Sec. VII, we show the results of nonexhaustive and unsuccessful attempts to explain the data by application of diffraction models and the distorted-wave Born-approximation method.

II. THEORY OF THE MEASUREMENTS

The theory of angular correlations of nuclear radiations has been treated extensively in the literature. We will review only those features which are relevant to inelastic α-particle scattering from 0^+ to 2^+ states. Our approach is essentially the same as that of Cramer and Eidson,[16] but we will make a few changes to fit our particular needs.

The wave function of an excited nuclear state with total angular momentum J where the m substates are degenerate is

$$\Psi_J = \sum_m a_m \exp(i\epsilon_m)\psi_{Jm}, \tag{1}$$

where $a_m \exp(i\epsilon_m)$ is the complex amplitude of the substate with angular momentum projection m, and ψ_{Jm} is the wave function of the substate with quantum numbers J and m. The complex amplitudes for a given reaction are functions of the scattering angle ϕ_α.[17]

The normalization of Eq. 1 requires that

$$\sum_m (a_m)^2 = 1. \tag{2}$$

The partial differential cross section to the mth substate is then

$$\sigma_m = (d\sigma/d\Omega)_m = (a_m)^2 (d\sigma/d\Omega)_J, \tag{3}$$

where $(d\sigma/d\Omega)_J$ is the usual differential cross section to the excited state with angular momentum J.

For our purposes, the axis of quantization is defined perpendicular to the reaction plane, and lies in the z direction as specified by $\mathbf{k}_i \times \mathbf{k}_f$, where $\mathbf{k}_i$ and $\mathbf{k}_f$ are the incident and final α-particle wave vectors, respectively, in agreement with the Basel convention. The full coordinate system is shown in Fig. 1. In this system and for α particles exciting a 0^+ to 2^+ transition, the symmetry theorem of Bohr[18] states that $a_{+1} = a_{-1} = 0$.

The angular correlation function[19] describing the emission of quadrupole γ rays with circular polarization λ in a $2^+ \rightarrow 0^+$ transition is

$$\begin{aligned} W^\lambda(\theta, \phi, \phi_\alpha) = (5/32\pi)\ \sin^2\theta \{ & (a_{+2})^2 (1+\lambda\cos\theta)^2 \\ & + 6(a_0)^2 \cos^2\theta + (a_{-2})^2 (1-\lambda\cos\theta)^2 - 2(6)^{1/2} a_0 a_{+2} \\ & \times (\cos\theta + \lambda)\ \cos\theta \cos(2\phi - \delta_0) - 2a_{+2}a_{-2} \sin^2\theta \\ & \times \cos(4\phi - \delta_2) - 2(6)^{1/2} a_0 a_{-2} \\ & \times (\cos\theta - \lambda)\ \cos\theta \cos[2\phi - (\delta_2 - \delta_0)] \}. \end{aligned} \tag{4}$$

The relative phases δ_i are related to the phases of the wave functions of Eq. (1) by the relations

$$\delta_0 = \epsilon_{+2} - \epsilon_0 \quad \text{and} \quad \delta_2 = \epsilon_{+2} - \epsilon_{-2}. \tag{5}$$

For right circularly polarized radiation (spin parallel to $\mathbf{k}$) $\lambda = +1$, and for the left circularly polarized radiation $\lambda = -1$, which is the converse of the older optical convention.

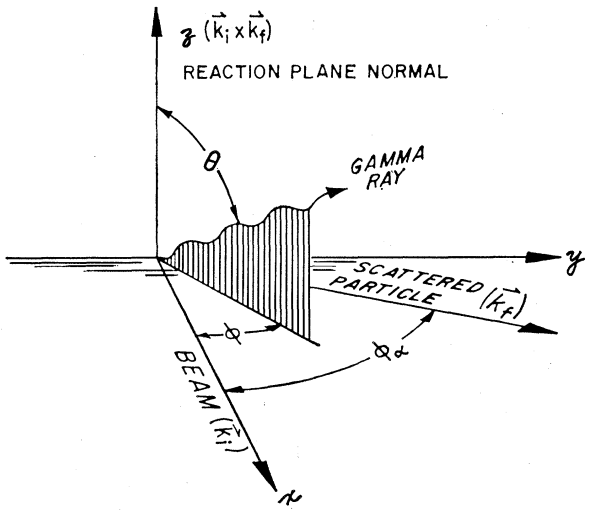

FIG. 1. Definition of coordinate system. The z axis is in conformity with the Basel convention.

[14] Provided by a National Science Foundation grant.
[15] J. S. Blair (private communications).
[16] J. G. Cramer, Jr., and W. W. Eidson, Nucl. Phys. **55**, 593 (1964).
[17] Our a_m are related to a_2 in Cramer and Eidson (Ref. 16) by the relation $(a_{+2})/(a_{-2}) = (a_2)$. We perfer the moduli of the amplitudes because these are the quantities measured.
[18] A. Bohr, Nucl. Phys. **10**, 486 (1959).
[19] T. D. Hayward, Ph.D. thesis, University of Washington, 1969 (unpublished).

When the polarization is not detected the correlation function is obtained by summing over λ, so that

$$W(\theta, \phi, \phi_\alpha) = \sum_\lambda W^\lambda(\theta, \phi, \phi_\alpha). \quad (6)$$

The polarization-insensitive normalized angular correlation function in the reaction plane ($\theta=\pi/2$) is obtained from Eqs. (4) and (6). The result[20] is

$$W(\pi/2, \phi, \phi_\alpha) = (5/16\pi)\{(a_{+2}-a_{-2})^2 + 4a_{+2}a_{-2}\sin^2 2[\phi-(\delta_2/4)]\}. \quad (7)$$

Equation (7) can be compared with the more common expression

$$W(\pi/2, \phi, \phi_\alpha) = A + B\sin^2 2(\phi-\phi_0). \quad (8)$$

In most previous experiments of α scattering the normalization of the "in-plane" angular correlation functions has not been determined, and only the A/B ratios [which are related to the ratios $(a_{+2}/a_{-2})^{\pm 1}$], and the relative phase $\phi_0=(\delta_2/4)$, were measured. On the other hand, Eq. (7) shows that values for a_{+2} and a_{-2} can be determined by use of a calibrated γ detector; however, because of the symmetric way these two parameters enter, it is impossible to distinguish the two values from one another. From Eq. (2), $(a_0)^2 = 1-\sum(a_{\pm 2})^2$. Thus, all three substate amplitudes, and the phase δ_2, can be found.

Figure 2 depicts the pure quadrupole radiation patterns. The $m=\pm 1$ is not present for α-particle scattering. The $m=0$ radiation is "missing" from the in-plane correlation, and its intensity is found by subtraction.

The ambiguity in the parameters a_{+2} and a_{-2} can be resolved[16,20] by a measurement of the circular polarization of the deexcitation γ rays. The circular polarization is the number of right circularly polarized γ rays minus the number of left circularly polarized γ rays divided by their sum, and is given by

$$P_c(\theta, \phi, \phi_\alpha) = \frac{W^{+1}(\theta, \phi, \phi_\alpha) - W^{-1}(\theta, \phi, \phi_\alpha)}{W^{+1}(\theta, \phi, \phi_\alpha) + W^{-1}(\theta, \phi, \phi_\alpha)}. \quad (9)$$

It is more convenient to average $P_c(\theta, \phi, \phi_\alpha)$ over ϕ.

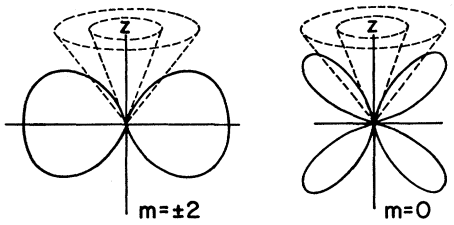

FIG. 2. Pure $l=2$ multipole radiation patterns. The $m=\pm 1$ are not excited in $0^+ \rightarrow 2^+$ excitation by α particles. The dashed lines indicate the two cones between which γ rays are accepted by the polarimeter.

[20] F. H. Schmidt, R. E. Brown, J. B. Gerhart, and W. A. Kolasinski, Nucl. Phys. **52**, 353 (1964).

The result is

$$\langle P_c(\theta, \phi_\alpha)\rangle = \frac{2\cos\theta[(a_{+2})^2-(a_{-2})^2]}{[(a_{+2})^2+(a_{-2})^2][1+\cos^2\theta]+6a_0^2\cos^2\theta}. \quad (10)$$

Equation (10) shows that a measurement of the sign of $\langle P_c\rangle$ is sufficient to resolve the ambiguity between the a_{+2} and the a_{-2}.

If it is assumed that a_{+2} and a_{-2} vary with the α-particle scattering angle in a continuous fashion, and if a_{+2} and a_{-2} are not equal at more than a few angles, determination of the sign of the circular polarization at only a few angles[16] will suffice to remove the ambiguity in all of the measured values of a_{+2} and a_{-2}.

From the preceding discussion, it is clear that measurements of the normalized in-plane angular correlation in conjunction with the measurements of the γ-ray circular polarization determine a_{+2}, a_{-2}, a_0, and δ_2. The only parameter which is not determined from such a set of measurements is the relative phase δ_0, which can be determined by observing the angular correlation out of the reaction plane, at, for example, $\theta=\pi/4$. We have not performed this measurement.

If $a_{+2}\neq a_{-2}$, the residual excited nuclei are polarized; the nuclear polarization is given by

$$P_n = (a_{+2})^2-(a_{-2})^2. \quad (11)$$

It should be pointed out that the form of the angular correlation is independent of any nuclear model. It depends only on the conservation of angular momentum, parity, and the properties of the electromagnetic field, while the information about the nuclear interaction is contained entirely within the complex amplitudes. The one-to-one correspondence between the quantum numbers and amplitudes describing the nuclear excited state and those describing the quadrupole radiation is due to the spherical symmetry of the ground state.

III. EXPERIMENTAL EQUIPMENT

A. Beam and Scattering Equipment

α particles were accelerated by the University of Washington FN Tamden Van de Graaff Accelerator.[14] The energy spread of the beam was about 6 keV. The beam current to the target ranged from a few nA to 2 μA, as required by counting rate considerations.

Targets, particle and γ-ray detectors, the polarimeter, and other equipment were located in a 60-in.-diam scattering chamber. It is equipped with four rotating elements, each of which can be positioned remotely. These are two arms on which detectors may be placed, a central target mount, and a circular floor for the support of heavy apparatus. A large port is located at the center of the chamber lid. The polarimeter was mounted through this port.

A 3-mm-diam tantalum defining aperture for beam

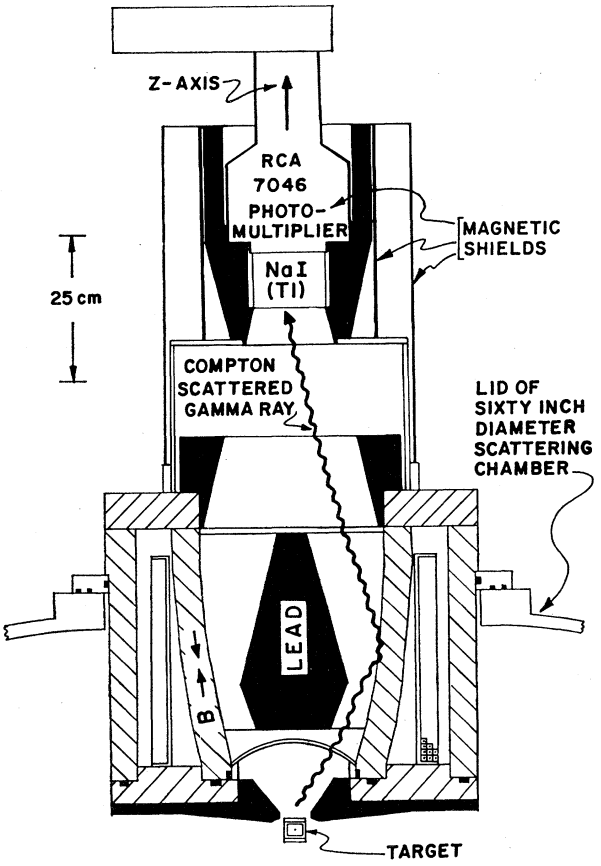

FIG. 3. Cross-sectional view of the γ-ray polarimeter. The solid sections are lead shielding; and the cross-hatched sections are magnetized iron. The interior iron surface is shaped to minimize data collection time (Ref. 22). The rectangular solid sections are rubber vacuum seals. γ rays enter the polarimeter through a $\frac{1}{16}$-in.-thick spherically shaped aluminum window below the central lead shield.

alignment was located 15 cm upstream from the target. It could be positioned on the beam axis or withdrawn from the beam path by remote control. The transmission through this aperture was $>85\%$. The aperture was withdrawn during all data collection. The reduction in γ-ray background radiation achieved by this technique was essential for the polarization measurements and helpful for the in-plane correlation measurements.

All portions of the scattering chamber which conceivably could be struck by stray beam were made of, or shielded with, lead or tantalum. Since the Coulomb barrier of these elements is higher than the incident α-particle energy, the γ-ray background associated with the beam was further reduced.

After passing through the target the beam was stopped in a Faraday cup lined with lead and located 3 m downstream. The cup was surrounded by a large neutron and γ-ray shield. Beam current entering the cup was integrated, converted to digital information, and displayed on a scalar indicating directly in μC.

B. Particle Detectors

The scattered α particles were detected in lithium-drifted silicon detectors placed 10 cm from the target. Rectangular apertures limited the acceptance of the detectors to 2° and 8.5° in the ϕ and θ directions, respectively. The detectors were cooled by liquid nitrogen in order to decrease the noise level and thereby provide better time resolution. The energy resolution of the detectors for 22.7-MeV α particles was $\approx$50 keV for reasonable counting rates.

C. γ-Ray Detector

γ rays were detected in a 4×4-in. NaI(Tl) crystal mounted on an RCA 7046 photomultiplier tube. For the in-plane correlation measurements, the detector was placed in a lead shield. The assembly was accurately positioned on the floor of the scattering chamber.

In order to normalize the in-plane angular correlation, the absolute efficiency of the γ-detector assembly was measured for 4.44-MeV radiation as a function of the lower pulse-height threshold to an accuracy of $\pm 3\%$. Details of the method are discussed in Appendix I of Ref. 20, and the most recent efficiency measurements, which employed the $^{12}C(p, p'\gamma)$ reaction at 6.140 MeV, are described in Ref. 21.

D. γ-Ray Polarimeter

Figure 3 is a cross-sectional view of the polarimeter. The polarimeter is based on the fact that the Compton-scattering cross section in the forward direction is larger when the electron spins of magnetized iron and the rotational sense of the incident photon are approximately antiparallel.[22]

The polarimeter consists of a circularly-symmetric magnetized-iron scatterer. The saturated iron provides a scatterer with $\approx 8\%$ of the electrons aligned. The interior surface of the polarimeter is shaped to minimize data collection time.[22] γ rays from the target with polar angles between 20° and 37.5° strike the iron wall of the polarimeter and some of them are Compton-scattered into the γ-ray detector (Sec. III C). The transmission of the polarimeter is $\approx 0.33\%$. Direct radiation from the target is prevented from reaching the detector by a lead shield located on the axis of the polarimeter. The transmission of 4.44-MeV γ rays through this shield is $\approx 0.001\%$; the background contribution is therefore negligible.

As shown in Fig. 3, the polarimeter is inserted through a 51-cm-diam opening in the lid of the scattering chamber, its axis coincides with the positive (negative) z axis for α particles scattered to the left (right)

[21] Annual Report, Nuclear Physics Laboratory, University of Washington, 1968 (unpublished).

[22] R. M. Steffan and H. Fraunfelder, in *Alpha-, Beta-, and Gamma-ray Spectroscopy*, edited by Kai Siegbahn (North-Holland Publishing Co., Amsterdam, 1965), Vol. 2, p. 1456.

of the beam. The circular polarization is inferred from the asymmetry in the transmission of γ rays in coincidence with inelastically scattered α particles for the two directions of the magnetic field. The asymmetry is defined as

$$A=2(T_{-}-T_{+})/(T_{-}+T_{+}), \tag{12}$$

where T_{+} and T_{-} are the transmissions of the polarimeter with the electron spins approximately parallel, and antiparallel, respectively, to the positive z axis.

The transmissions are proportional to the values of $W^{\lambda}(\theta, \phi, \phi_{\alpha})$ of Eq. (4), averaged over the acceptance angles of the polarimeter. The proportionality factor depends upon the geometrical shape of the polarimeter scattering surface and the Compton scattering cross section. The result[19] for our polarimeter is

$$A\cong(0.11)[(a_{+2})^2-(a_{-2})^2][(a_{+2})^2 +(a_{-2})^2+2.53(a_0)^2]^{-1}. \tag{13}$$

Multiple scattering effects are not included in the calculation.

E. Targets

The targets were self-supporting natural-carbon foils mounted on aluminum frames. For the excitation function measurements (Sec. IV) a 40-μg/cm^2-thick foil was used; whereas for the angular correlation and circular polarization measurements, 197-μg/cm^2-thick foils were used. The uncertainties in the target thicknesses are $\pm 10\%$.

F. Electronic Equipment

Figures 4 and 5 are simplified pictorial diagrams of the circuits used for the correlation and for the polarization measurements, respectively. Only one of the two α-counter channels is shown. A "fast" and a "slow" preamplifier was connected to each α detector. Differentiated fast pulses (rise time $\approx$7 nsec) were obtained by the transformer coupling technique described by Williams and Biggerstaff.[23] Both preamplifiers were mounted inside the scattering chamber close to the detectors to minimize noise pickup. For the γ detector, fast-rise pulses were obtained from the anode and delay-line-shaped. Integrated "slow" pulses for pulse-height discrimination were taken from the tenth dynode.

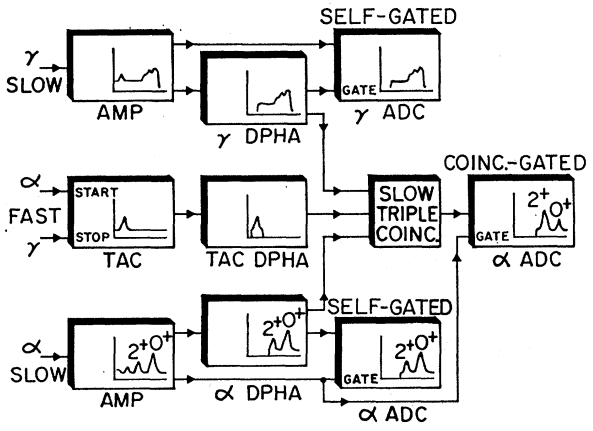

FIG. 4. Simplified schematic of electronic circuit for the in-plane angular-correlation measurements. Two α detectors were used, but only one α channel is shown. All analog-to-digital converters (ADC) were interfaced on-line to an SDS 930 computer.

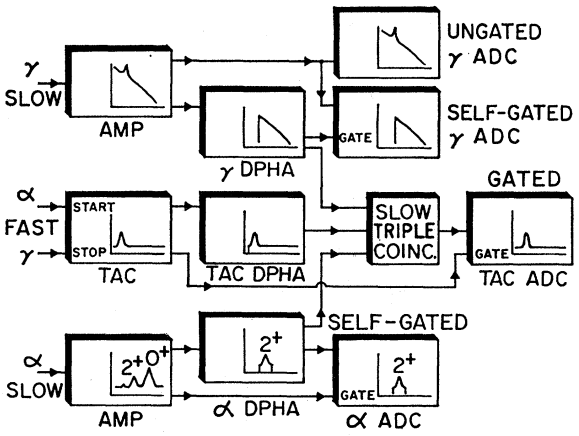

FIG. 5. Simplified schematic of electronic circuit for the circular polarization measurement. Two α-particle channels were used. The accidentals were obtained from the time-to-amplitude converters (TAC) spectra. All analog-to-digital converters (ADC) were interfaced on-line to an SDS 930 computer.

The fast signals indicated on Figs. 4 and 5 were derived from tunnel diode discriminators operating on the leading edge of the pulses from the fast preamplifiers. The discriminator outputs were appropriately delayed and fed to a time-to-amplitude converter (TAC). The coincidence peak in the time spectrum was about 4 nsec wide at half-maximum.

The integrated slow pulses were passed through amplifiers and selected by differential pulse-height analyzers (DPHA's). The signals from the DPHA's operated both a triple coincidence circuit and linear gates at the input to analog-to-digital converters (ADC's). The latter were interfaced to a Scientific Data Systems computer (SDS 930) which stored the several spectra. Thus, as indicated by the diagrams in Fig. 4, only the relevant portions of the raw pulse spectra were analyzed, stored, and displayed.

The TAC spectrum was utilized in two different ways. For the in-plane correlations, a DPHA selected the coincidence peak. The DPHA output then triggered the triple coincidence circuit, as shown in Fig. 4. Accidental coincidences between elastically scattered α particles and γ rays thus appear in the coincidence-gated α-particle spectrum. The number of accidentals occurring in the inelastic α peak is in the ratio of the inelastic-to-elastic cross sections. The "self-gated" α spectrum contains the required cross-section data.

[23] C. W. Williams and J. A. Biggerstaff, Nucl. Instr. Methods **25**, 370 (1964).

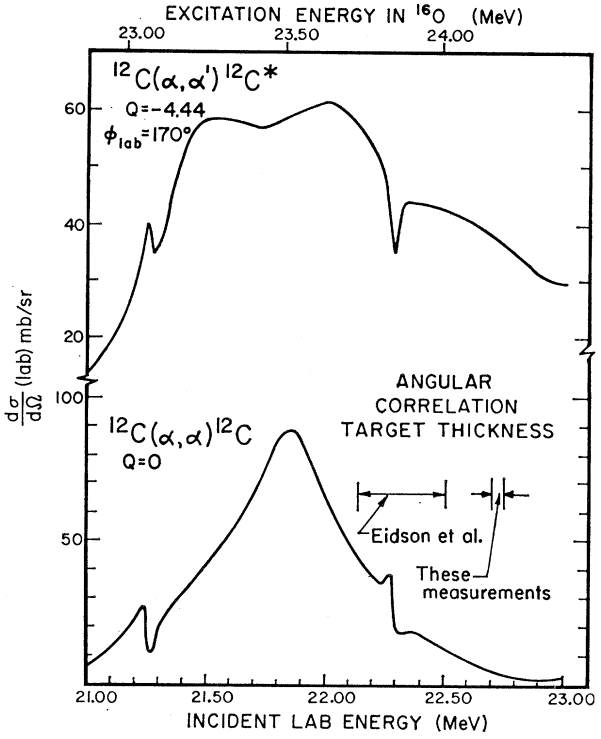

FIG. 6. Excitation functions for the ground and first excited states. A beam energy of 22.750 MeV was selected for the subsequent angular correlation and polarization studies.

Figure 5 depicts the TAC mode of operation for the polarization measurements. The DPHA's following the α-detector amplifiers are adjusted to select only the inelastic peak, and the DPHA on the TAC accepts most of the time spectrum. The final time spectrum, gated by the triple coincidence, thus contains accidental counts which satisfy all criteria except time coincidence. The peak of this spectrum contains the true coincidences, and the continuum contains the accidentals. Since the time over which the accidentals are measured is about 200 nsec, compared with about 10 nsec for the peak, the accidental background under the peak is determined to a high degree of accuracy.

One further essential feature to notice about both circuits is the role played by the γ-detector DPHA, and the ungated and self-gated γ spectra. The γ rays entering the polarimeter produce positron-electron pairs as well as undergoing Compton scattering. The annihilation radiation thus generated does not exhibit an asymmetry with field direction. It is therefore necessary to set the lower discriminator level on the "slow" γ signal above 0.5 MeV, as indicated in Fig. 5. In addition, short-lived positron activities were generated in the target, so for both experiments the 0.5-MeV radiation was harmful and thereby excluded. On the other hand, the ungated spectrum, which included the 0.5-MeV peak, provided a constant monitor of the gain of the γ detector.

Numerous scalers were employed at various points in the circuits as monitors. Each scaler was read by the computer and the information printed by a line printer. For the polarization experiment it was absolutely essential that all equipment operate with great stability in order to achieve consistent results.

IV. SELECTION OF INCIDENT ENERGY

In the Introduction, it was pointed out that we were stimulated by the angular correlation studies of Eidson *et al.*[10] at 22.5 MeV. Nevertheless, as a preliminary step, it was deemed wise to examine the excitation functions of α particles scattered from ^{12}C, since these measurements could not be done conveniently by the Indiana group.[10] The excitation functions were measured for the elastic $^{12}C(\alpha,\alpha)^{12}C$ and inelastic $^{12}C(\alpha,\alpha)^{12}C^*$ (2^+, 4.44-MeV) reactions at laboratory scattering angles of 90°, 165°, and 170°, and at $\approx$100 energy values in the range from 21.000 to 23.000 MeV. The energy loss in the target was $\approx$10 keV (40 μg/cm^2). The increments varied from 10 to 40 keV depending upon the amount of structure observed in the cross sections.

Figure 6 shows the excitation functions for the two reactions at 170°. Statistical errors of most of the data points are less than the line thicknesses. These cross sections are typical of what is found at the other angles.[19] Three resonancelike structures are clearly indicated at incident energies of 21.28, 21.9, and 22.32 MeV. The widths are about 25, 450, and 30 keV, respectively. These resonances have also been observed by Morgan *et al.*[24]

The energy spreads of the targets employed by Eidson *et al.*,[10] and by us for the correlation and polarization measurements, are indicated on Fig. 6. Clearly, 22.5 MeV might have been a poor choice for our studies. At 22.750 MeV, however, the cross sections are reasonably free of resonance structure. Although higher energy might be desirable, 22.750 MeV is within the range attainable by our Tandem Van de Graaff over long periods of steady operation. For these reasons, we chose 22.750 MeV.

V. DATA COLLECTION AND ANALYSIS

A. In-Plane Angular Correlations

We define a *measured* angular correlation function W_F, which is related to the in-plane function Eq. (7) by

$$W_F(\pi/2,\phi,\phi_\alpha)=(2\Delta\phi)^{-1}\int_{\phi-\Delta\phi}^{\phi+\Delta\phi}W(\pi/2,\phi,\phi_\alpha)\,d\phi, \tag{14}$$

[24] J. F. Morgan, R. K. Hobbie, and N. M. Hintz, J. Phys. Soc. Japan **24**, 341 (1968); Annual Report, John H. Williams Laboratory of Nuclear Physics, University of Minnesota, 1967 and 1968 (unpublished); J. F. Morgan, Ph.D. thesis, University of Minnesota, 1969 (unpublished).

where $\Delta\phi$ is the half-angle subtended by the γ-detector assembly in the ϕ direction. No corrections were applied in the θ direction. Next, Eq. (7) can be expressed in an obvious linear form; similarly, the linear form of Eq. (14) is

$$W_F(\pi/2, \phi, \phi_\alpha) = A_1 + KA_2 \cos 4\phi + KA_3 \sin 4\phi, \quad (15)$$

where K is a correction factor for the finite angular acceptance of the γ detector. The linear form of Eq. (7), together with Eqs. (14) and (15), yield the following results:

$$K = (\sin 4\Delta\phi)/(4\Delta\phi), \quad (16)$$

$$\delta_2 = \tan^{-1}(A_3/A_2), \quad (17)$$

$$(a_0)^2 = 1 - (16\pi/5)A_1, \quad (18)$$

and

$$(a_{\pm 2})^2, (a_{\mp 2})^2 = (8\pi/5)\{A_1 \pm [A_1^2 - (A_2^2 + A_3^2)]^{1/2}\}. \quad (19)$$

The two solutions given in Eq. (19) are the unidentified values of $(a_{+2})^2$ and $(a_{-2})^2$. K is a function of the γ-ray collimator angle, and is equal to 0.96.

The measured correlation function W_F is related to the true number of α-γ coincidences C, by the equation

$$W_F = C/[N_{\alpha'}(f\epsilon\Omega)], \quad (20)$$

where $N_{\alpha'}$ is the number of inelastically scattered α particles, f is the fraction of the total pulse spectrum accepted by the γ DPHA (Fig. 4), ϵ and Ω are the total efficiency and the solid angle of acceptance of the γ detector, respectively. Because of Compton scattering and penetration in the walls of the lead γ-ray collimator, Ω cannot be calculated accurately. However, the effective value of Ω can be found by the method discussed in Appendix I of Ref. 20, with the modifications mentioned in Ref. 21. For each data run, the average value of f was determined from the self-gated γ spectrum as displayed by the computer. Gain shifts due to high and variable γ-counting rates were therefore taken into account.

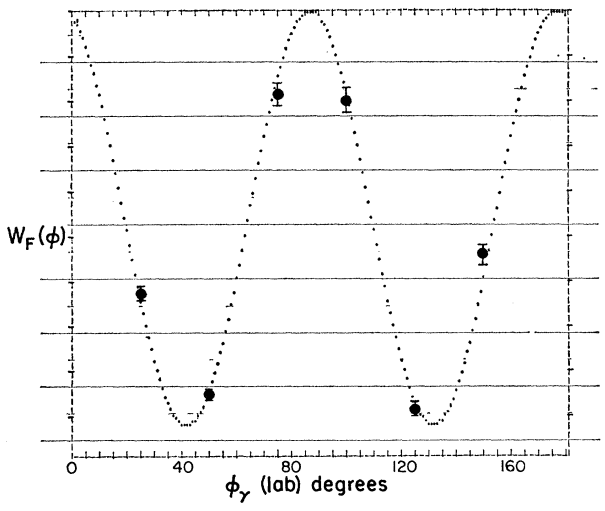

FIG. 7. Typical angular correlation data fit by Eq. (15). The plot is directly from the computer. Scattering angle 85.56° (c.m.).

The coincidences of Eq. (20) must be found from the *measured* number of coincidences (the coincidence-gated inelastic peak) $C_{\alpha'}$ by the relation

$$C = C_{\alpha'} - (C_\alpha N_{\alpha'})N_\alpha^{-1}, \quad (21)$$

where C_α is the number of accidental coincidences between elastically scattered α particles, N_α, and γ rays. In addition, each quantity was corrected for counting losses in both the fast and slow circuits due to finite pulse-pair resolution.

At each of 35 α-detector angles the correlations were determined at six γ-ray angles. Equation (15) was then fit by a least χ^2 computer program to the measured points. A typical set of correlation data and the computer fit are shown in Fig. 7.

The $(a_m)^2$ and relative phase δ_2 were then calculated from Eqs. (17)–(19). The error in each parameter was determined by a finite difference calculation. The error in the parameter P is given by

$$\delta P = [\sum_i (P - P_i)^2]^{1/2}, \quad (22)$$

where P_i is the value of P obtained by increasing the correlation at the ith γ angle by its error, and the sum runs over all γ angles of a particular angular correlation. The error in each correlation measurement included the statistical error and the error in the γ-ray detector calibration.

B. γ-Ray Circular Polarization

In Sec. III D, it was pointed out that the transmission of the polarimeter is about 0.33%. Although the solid angle of acceptance of the polarimeter is 0.91 sr, and the in-plane γ-detector solid angle is 0.030 sr, the intensity of γ radiation, as exhibited by the $m = \pm 2$ polar diagram of Fig. 2, is much less over the acceptance cone of the polarimeter than it is in the reaction plane. Consequently, the true coincidence rate for the polarization measurement was distressingly low, and the relative magnitude of the accidental coincidence background more critical than for the in-plane measurements. Furthermore, the expected asymmetries are only a few percent, so that a large number of true coincidences were required in order to obtain meaningful statistical results.

The true number of coincidences, C, for a data run was measured by analysis of the α-γ coincidence time spectrum, as generated by the TAC, and displayed by the computer (cf. Sec. III F). The result is given by

$$C = \sum_p N_t - (p/b) \sum_b N_t, \quad (23)$$

where N_t are the counts in the tth time channel, and p and b are the number of time channels in the coincidence

TABLE I. Data from two typical polarization runs (of 16) at 115° (lab).

Integrated beam μC	Polarimeter electron spin	Length of run (sec)	Total γ slow counts	Total inelastic α counts Right	Left	Total counts time peak $(\Sigma_p N_t)$ Right	Left	True coincidences Right	Left	Average asymmetry $\langle A \rangle$
4000	up	2769	8.26×10^6	7.78×10^6	7.80×10^6	981	957	720±31	666±31	
4000	down	2536	8.18×10^6	7.61×10^6	7.74×10^6	947	1018	672±31	705±32	+0.064±0.038

peak and in the flat background, respectively. The statistical error in C is then

$$C=[\sum_p N_t+(p/b)^2\sum_b N_t]^{1/2}. \quad (24)$$

Typical data runs at $\phi_\alpha=115°$ (lab) for the two directions of the polarimeter magnetization are tabulated in Table I.

Two α-particle detectors were set at equal scattering angles, one to the right and one to the left of the beam direction. Although the detectors were made as identical as possible with respect to solid angle subtended, efficiency, angular setting, and resolution, the counting rates in the two differed by several percent, as is apparent in Table I. Moreover, the gain of the γ detector depended upon the field direction and exhibited a kind of unpredictable hysteresis effect. (Note the two γ counts in Table I.) It was therefore essential to define the asymmetry in a manner which is very little affected by extraneous differences between left (L), right (R), or electron spin up (U), down (D). It can be shown[19] that the following expression for the average asymmetry indeed fulfills these requirements:

$$\langle A\rangle=(T_{LD}-T_{RD})/(T_{LD}+T_{RD}) +(T_{RU}-T_{LU})/(T_{RU}+T_{LU}), \quad (25)$$

where the T's are the four values of the transmission of the polarimeter for coincident α-γ events. The T's are proportional to the corresponding C's of Eq. (23). For the extraneous differences in the α and γ detectors, the resultant error in $\langle A\rangle$ cannot exceed 10% in these measurements. The statistical error in $\langle A\rangle$ was calculated from the statistics of the coincidences.

A total of about 22 000 true coincidences was collected for the measurement at 115°. The magnetic field was reversed 16 times. Accelerator operation time was about 30 h.

The average asymmetry, together with its error, was calculated by the computer and displayed as an "updated" result at the end of each data run. The display was used to determine when sufficient data had been collected for a particular polarization measurement.

IV. EXPERIMENTAL RESULTS

A. Differential Cross Sections

The elastic and inelastic (2^+, 4.44-MeV) differential cross sections were measured at 35 scattering angles as

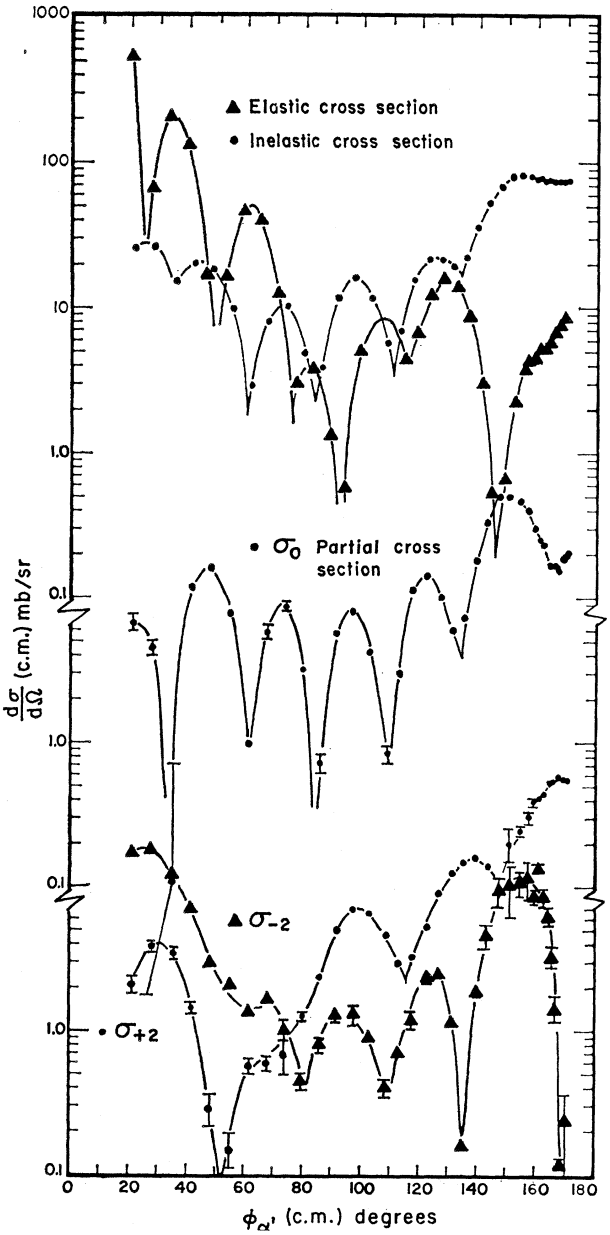

FIG. 8. The top two curves are the elastic and inelastic cross sections for $^{12}C(\alpha, \alpha)^{12}C$ and $^{12}C(\alpha, \alpha')^{12}C^*$ (4.44, 2^+), respectively. The middle curve is the partial inelastic cross section for excitation of the $m=0$ substate, and the lower two curves are these cross sections for the $m=+2$ and -2 substates. The lines are drawn to assist the eye.

a by product of the α-γ correlations (cf. Fig. 4). The results, exhibited at the top of Fig. 8, show the usual diffraction structure associated with α-particle scattering. The lines are drawn through the points as an aid to the eye. The maxima of the inelastic cross sections lie at approximately the minima of the elastic cross sections, especially for the first few oscillations, as predicted by the Blair phase rule.[4]

B. In-Plane Angular Correlations

A typical set of angular correlation data, and the computer fit to the experimental points, is shown in Fig. 7. The substate amplitude parameters $(a_0)^2$ and $(a_{\pm 2})^2$, calculated from Eqs. (18) and (19), are displayed in Fig. 9. The parameters $(a_0)^2$ and $(a_{\pm 2})^2$ exhibit an oscillatory character. The identification of $(a_{+2})^2$ and $(a_{-2})^2$, as shown on Fig. 9, is discussed in Sec. IV D. The relative phase angle δ_2 [cf. Eqs. (5) and (17)], between the $+2$ and the -2 substate wave functions, is shown in Fig. 10.

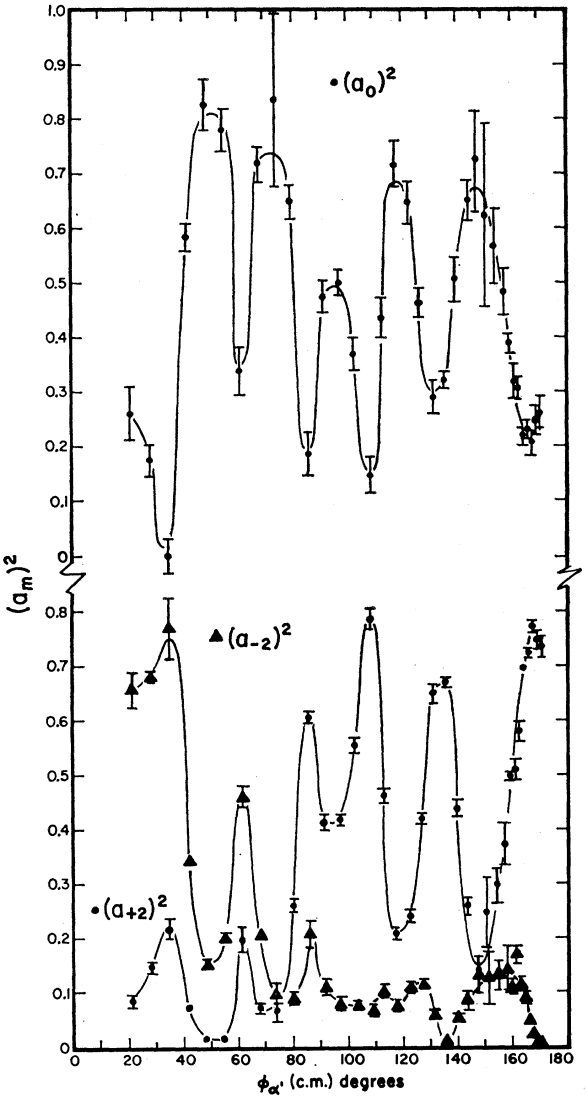

FIG. 9. The squares of the substate amplitudes. The ambiguity between $(a_{\pm 2})^2$ was resolved by determination of the circular polarization of the γ rays.

C. γ-Ray Polarization

With a knowledge of $(a_{\pm 2})^2$ and $(a_0)^2$, the expected magnitude of the circular polarization of coincident 4.44-MeV γ rays can be found from Eq. (10) as a function of the polar angle θ. The predicted magnitude of the asymmetry follows from Eq. (13); the results are shown in Fig. 11. The solid points, shown for both signs, are the predicted asymmetries. At two angles, 55° and 130° (lab), the asymmetry is $\approx$zero. If we assume that no discontinuities occur between the points at which measurements were made,[16] determination of the sign of the circular polarization at three angles only is sufficient to resolve all ambiguities between a_{+2} and a_{-2}. Accordingly, the asymmetry was measured at 25°, 115°, and 160°. These choices were dictated by taking into account both the expected asymmetries and the inelastic cross sections. In addition, a measurement was performed at 130°, where the polarization is approximately zero. The results of the four asymmetry measurements are shown as open circles on Fig. 11. Each point agrees with the predicted magnitude within statistical error. The solid line on Fig. 11 was then drawn through the remaining predicted asymmetries as an aid to the eye.

D. Partial Cross Sections and Nuclear Polarization

The signs of the γ-ray circular polarization leads to differentiation between the $(a_{+2})^2$ and the $(a_{-2})^2$. The values of these parameters, properly separated, are shown on Fig. 9.

The differential cross sections for inelastic scattering to each of the substates are then given by Eq. (3). These are displayed in the lower half of Fig. 8. The σ_0 has the most regular diffractionlike pattern. The first five minima are separated by $(24.8\pm 1.6)°$. Moreover, the σ_0 maxima and minima fall much more closely at the minima and maxima of the elastic cross section than do the maxima and minima of the total inelastic cross section. The σ_{-2} predominates over the σ_{+2} in the forward direction, whereas the reverse is true in the backward direction. Neither of these cross sections is so strikingly diffractionlike as is σ_0.

Finally, we show in Fig. 12 the polarization of the nuclei in the 2^+ excited state, as found from Eq. (11). In the forward direction, the nuclei spin in the sense expected for a collision of classical hard spheres with contact friction. At 75°, the polarization is zero and then becomes "anticlassical" for all larger angles investigated.

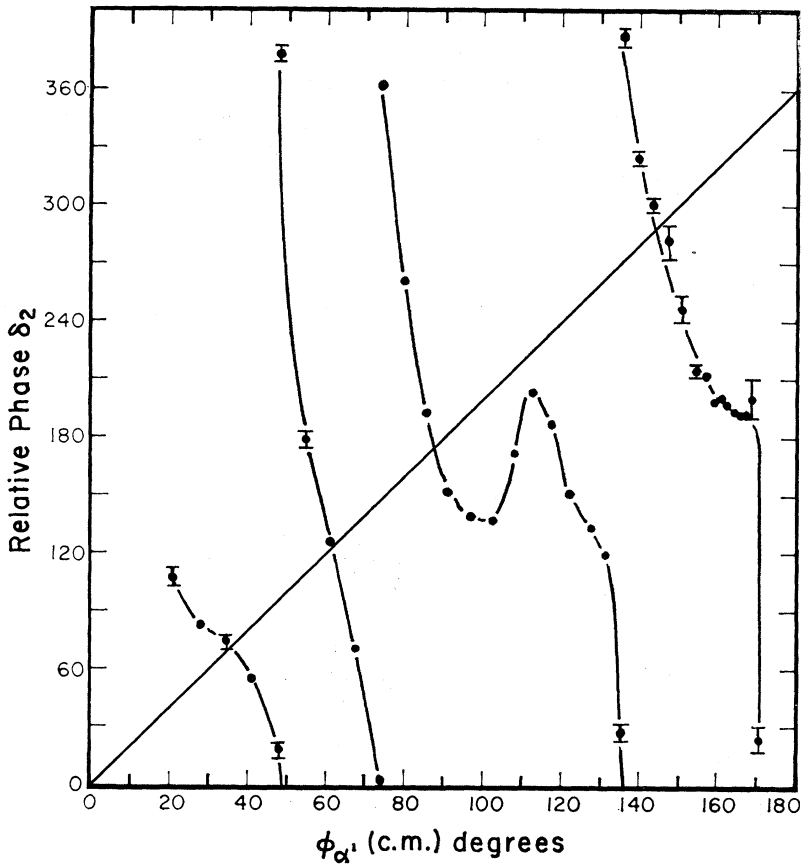

FIG. 10. Relative phase angle δ_2 between the $+2$ and -2 substates. The diagonal line is the adiabatic prediction.

VII. COMPARISONS WITH THEORETICAL MODELS AND DISCUSSION

A. General Comments

A satisfactory model of the inelastic scattering process should be capable of predicting each of the five parameters $a_{\pm 2}$, a_0, δ_2, δ_0, and the cross section. Hence, the demands imposed upon the model are stringent indeed. Moreover, since theories of inelastic scattering generally start with a correct interpretation of elastic scattering, the over-all expectations for the model are even greater.

Prospects for explanation of our data, which includes all parameters except δ_0, appear rather bleak. The reasons for discouragement include (1) direct interaction models of α scattering are generally more successful at energies higher than the 22.750 MeV employed here; (2) ^{12}C is well known to be a recalcitrant nucleus in so far as yielding readily to theoretical interpretation,[15] a view which is supported by recent failures[24] to fit elastic α scattering at 22.90 MeV with any reasonable model; (3) the excitation functions displayed in Fig. 6 by no means eliminate the possibility that our data is influenced by resonance effects, and the excitation functions found by the Minnesota group[24] extending up to 30 MeV are suggestive of Ericson fluctuations.

Despite the discouraging situation, we made several calculations to see if any trends could be discerned in a direction in agreement with our experimental results. In particular, the regularity of σ_0, Fig. 8, together with its agreement with the Blair phase rule,[4] would seem to offer the best hope. On the other hand, the general appearance of both σ_{+2} and σ_{-2} does not resemble the predictions of most theories. It is interesting to note that these cross sections tend to attenuate and shift the maxima and minima of the inelastic cross sections. One encouraging observation is that the elastic and inelastic angular distributions measured by Eidson *et al.*[10] at 22.5 MeV, and by Atneosen *et al.*[25] at 21.90, 22.48, and 22.73 MeV are all essentially the same as ours. In fact, the data of Eidson *et al.*[10] was evidently not seriously affected by the sharp resonance at 22.32 MeV, probably because of their spread in energy (see Fig. 6). These comparisons suggest that interference from this isolated resonance may not be severe.

B. Diffraction Models

As a first step, we applied the Fraunhofer diffraction model of Blair.[4] The only difference between the various

[25] R. A. Atneosen, H. L. Wilson, M. B. Sampson, and D. W. Miller, Phys. Rev. **135**, B660 (1964).

substates predicted by the model is in the magnitude of σ_0 as compared with $\sigma_{\pm 2}$. The only way the model can produce a different period in the oscillations, as is evident in the experimental data, is to choose a different value for the interaction radius for each substate, but there seems to be little theoretical basis[15] for assuming such differences. Nevertheless, if one takes kR values of 5.62, 6.10, and 7.35, for the substates $m=+2$, -2, and 0, respectively, the periods of the oscillations in the partial cross sections can approximately be matched. However, the predicted magnitudes bear little resemblance to the data.

We have not made quantitative comparisons with the ring-locus models of Inglis,[12] and of Verhaar and Tolsma.[12] However, these models make predictions concerning the behavior of the relative phase angle δ_2 of Fig. 10. The adiabatic theory of Blair and Wilets[26] predicts that $-\phi_0$ of Eq. (8) lies along the recoil axis; this corresponds to the diagonal line shown on Fig. 10. The ring-locus models predict that δ_2 should equal the adiabatic line at the maxima of the inelastic cross section. However, in our case, this would refer to the maxima of σ_{+2} and (or) σ_{-2}, since only these play a role in the phase δ_2. Comparison of Fig. 10 with the σ_{+2} and σ_{-2} of Fig. 8 does indeed bear this out to some extent. The experimental δ_2 crosses the adiabatic line first near a peak in both σ_{+2} and σ_{-2}. The next lies near what seems to be a tendency for a peak. The third is just below a peak in the σ_{+2}. For larger angles, little can be said.

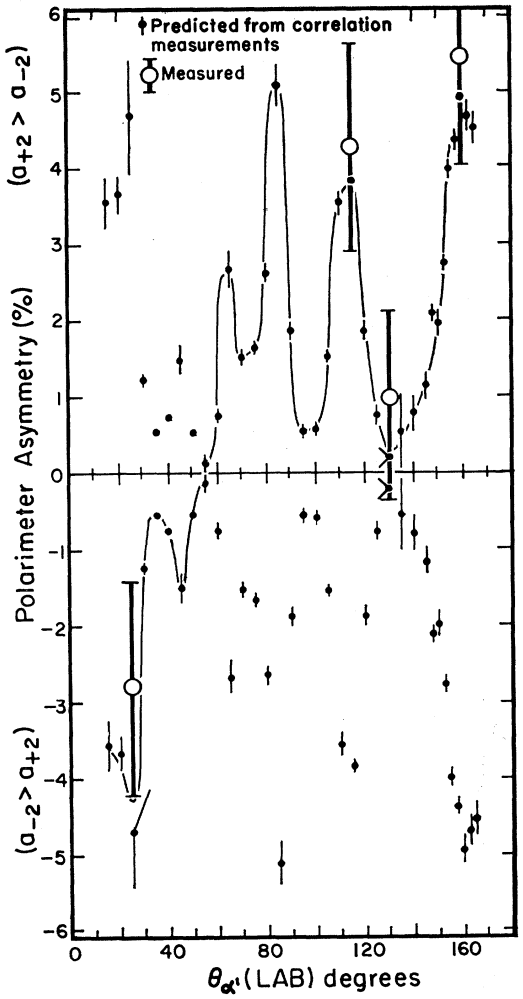

FIG. 11. The solid points are predicted polarimeter asymmetries. They are repeated for + and − values. The open points are the measured asymmetries. The line is drawn through the correct set of asymmetries to aid the eye.

[26] J. S. Blair and L. Wilets, Phys. Rev. **121**, 1493 (1961).

C. Distorted-Wave Born Approximation

Although attempts by Morgan *et al.*[24] to fit the elastic cross section at 22.90 MeV with the optical model were unsuccessful, we carried out a number of optical-model searches with our data to try to obtain a reasonable set of optical parameters. The parameters thus determined were used in a DWBA calculation of the σ_m to see if any hopeful trends might emerge.

For the optical-model calculation we employed the search code ABACUS-2.[27] The form of the optical potential used was

$$V_{\rm op}(r)=V_C(r)-Vf_1(r)+4iW_s(d/dr)f_2(r), \quad (26)$$

where $V_C(r)$ is the Coulomb potential of a uniformly charged sphere of radius R_c and charge Ze, V is the real potential, and W_s is the surface-imaginary potential. The form factors for the potentials are the Woods-Saxon type, given by

$$f_i(r)=\{1+\exp[(r-R_i)/a_i]\}^{-1}, \quad (27)$$

where the a_i are the surface diffuseness parameters. The nuclear radii are

$$R_i=R_{0i}A^{1/3}. \quad (28)$$

The best fit to the elastic cross section, obtained by searching over a limited range of the data (20° to 75° c.m.), is shown in Fig. 13. The parameters are $V=174$ MeV, $W_s=19.6$ MeV, $R_{0c}=R_{01}=1.44$ F, $R_{02}=1.88$ F, $a_1=0.38$ F, and $a_2=0.39$ F.

These predictions, like those of Morgan *et al.*,[24] are not particularly good; nevertheless DWBA calculations were performed with the code DWUCK.[28] The z axis for this code is along $\mathbf{k}_i$, and the y axis along $\mathbf{k}_i\times\mathbf{k}_f$.[29] The partial-wave amplitudes obtained from DWUCK were therefore rotated into our coordinate system, as

[27] E. H. Auerbach, ABACUS-2 (revised version), Brookhaven National Laboratory Report No. 6562, 1962 (unpublished).
[28] P. D. Kunz, DWUCK, University of Colorado, 1967.
[29] P. D. Kunz (private communication).

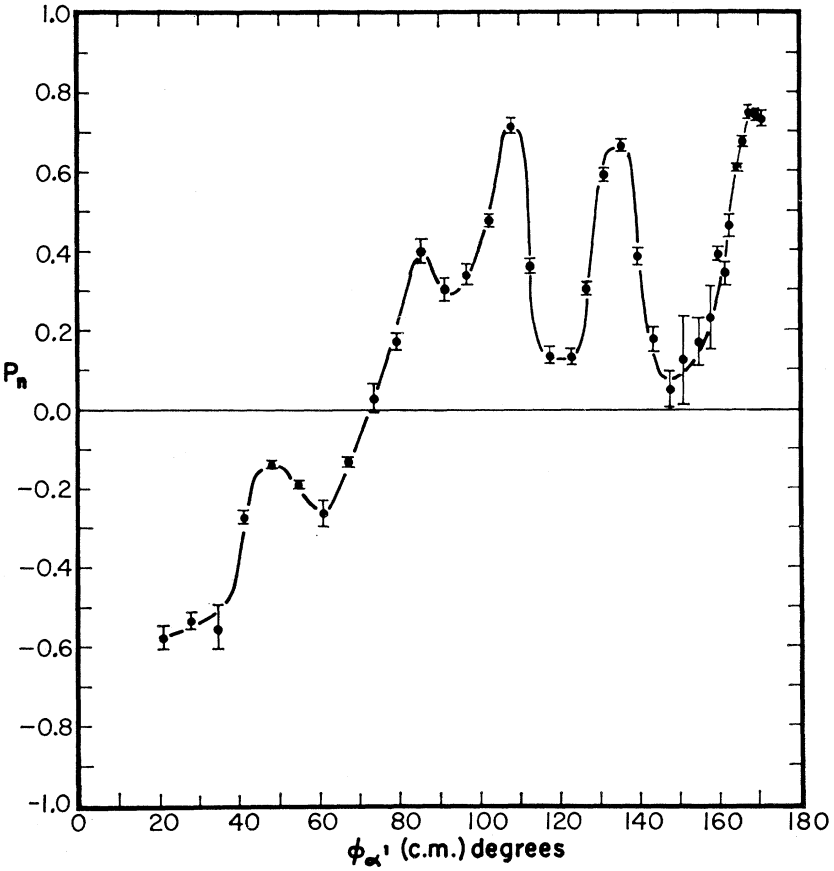

FIG. 12. Polarization of ^{12}C(4.44-MeV, 2^+) nuclei. In the forward direction, the nuclei spin as would scattering of classical hard spheres. For angles $>75°$, they spin as if the α particles went "behind" the ^{12}C and gave them a spin opposite to that of the classical type of collision.

shown in Fig. 1, and used to calculate the σ_m. The results are presented in Fig. 14. The agreement with the experimental data is very poor (see Fig. 8); however, there are two interesting features: (1) The period of the σ_0 is less than those of the $\sigma_{\pm 2}$, in agreement with the data; (2) the σ_{+2} and σ_{-2} differ from one another, but not nearly as much as the experimental values.

In principle, our experimental methods can be applied to nuclei other than ^{12}C, but success with ^{12}C does not assure success with different targets. So far as we can judge, any other nucleus would present more difficulty because of lower cross sections, more intense background radiations, and smaller separation between the states. Nevertheless, we intend to examine other nuclei. Unfortunately, while polarization seems to be the most interesting feature[30] it is obviously quite difficult to determine.

We no not feel competent to judge fairly whether the extensive efforts required for these experiments will actually lead to a better understanding of inelastic scattering, though we are inclined to believe that they could. Our opinion is based simply on the notion that

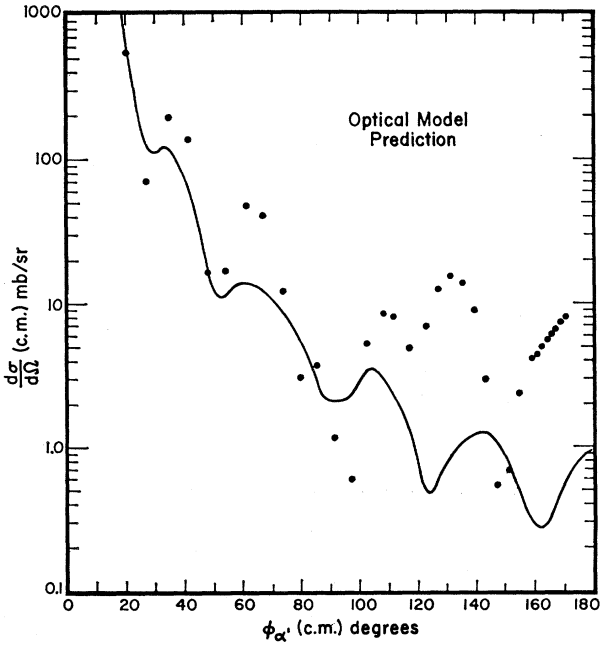

FIG. 13. Optical-model fit to the elastic differential cross section. The search was limited to the data between 20° and 75°.

[30] G. R. Satchler, Nucl. Phys. **16**, 674 (1960).

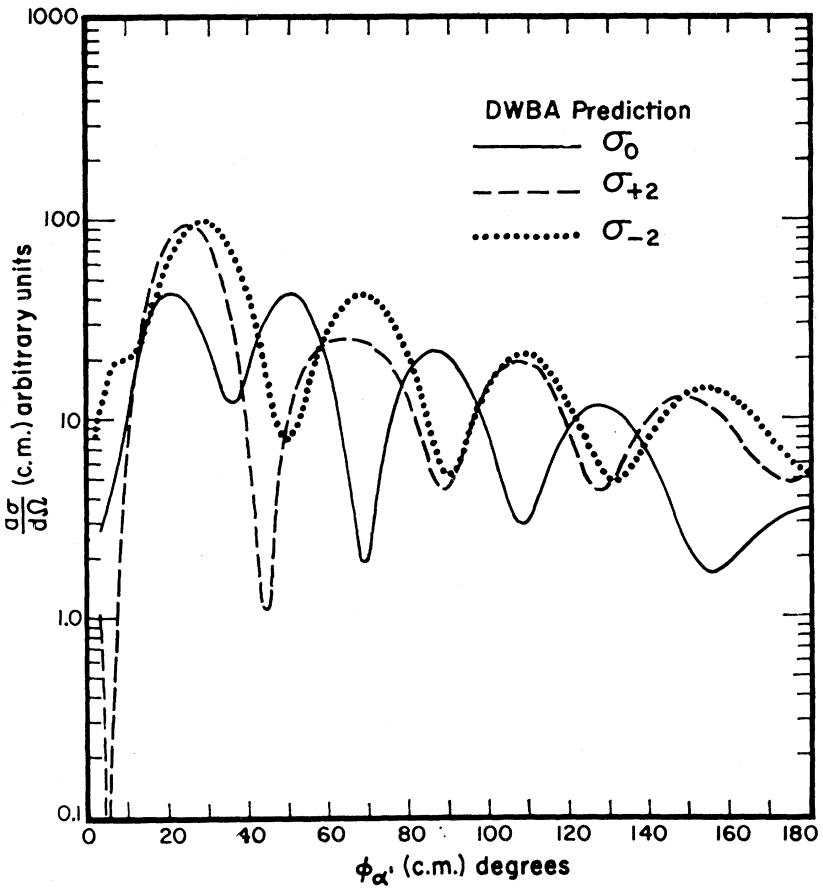

FIG. 14. DWBA calculations of the partial differential cross sections (σ_m). These are to be compared with the data of Fig. 8.

the more details one can determine, the better one is able to understand the whole.

ACKNOWLEDGMENTS

We wish to thank J. Eenmaa, T. K. Lewellen, R. H. Lewis, and J. R. Tesmer for their extensive assistance with data collection. We are especially appreciative to D. M. Patterson for the use of his data-collection computer programs, and to Professor J. B. Gerhart for his painstaking examination of the manuscript and calculations. We are grateful to Professors J. G. Cramer, J. S. Blair, and E. M. Henley for many helpful discussions and advice, and to Professor T. J. Morgan (deceased), Dr. W. G. Weitkamp, and other members of the staff of the University of Washington Nuclear Physics Laboratory for their valuable technical assistance.